

# Shortest Paths and Convex Hulls in 2D Complexes with Non-Positive Curvature

Anna Lubiw\*

Daniela Maftuleac\*

Megan Owen<sup>†</sup>

## Abstract

Globally non-positively curved, or CAT(0), polyhedral complexes arise in a number of applications, including evolutionary biology and robotics. These spaces have unique shortest paths and are composed of Euclidean polyhedra, yet many properties of convex hulls in Euclidean space fail to transfer over. We give examples of some such properties. For 2-dimensional CAT(0) polyhedral complexes, we give polynomial-time algorithms for computing convex hulls using linear programming and for answering shortest path queries from a given source point.

## 1 Introduction

Convex hulls and shortest paths—and algorithms to find them—are very well understood in Euclidean spaces, but less so in non-Euclidean spaces. We consider these two problems in finite *polyhedral complexes* which are formed by joining a finite number of  $d$ -dimensional convex polyhedra along lower dimensional faces. We will primarily be concerned with the 2D case of triangles or rectangles joined at edges.

We will restrict our attention to polyhedral complexes that are globally non-positively curved, or CAT(0). Introduced by Gromov in 1987 [23], CAT(0) metric spaces (or spaces of global non-positive curvature) constitute a far-reaching common generalization of Euclidean spaces, hyperbolic spaces and simple polygons. The initials “CAT” stand for Cartan, Alexandrov, and Toponogov, three researchers who made substantial contributions to the theory of comparison geometry. In a CAT(0) space, in contrast to a space of positive curvature, there is a unique geodesic (locally shortest path) between any two points and this property characterizes CAT(0) complexes.

The impact of CAT(0) geometry on mathematics is significant especially in the field of geometric group theory where the particular case of CAT(0) polyhedral complexes formed

---

\*David R. Cheriton School of Computer Science, University of Waterloo, Waterloo, Ontario N2L 3G1, Canada, alubiw@uwaterloo.ca, daniela.maftuleac@uwaterloo.ca; † Department of Mathematics and Computer Science, Lehman College, City University of New York, United States, megan.owen@lehman.cuny.edu

by cubes—the so-called “CAT(0) cube complexes”—are particularly relevant [10, 23, 26]. Most of the work on CAT(0) metric spaces so far has been mathematical. Algorithmic aspects remain relatively unexplored apart from a few results for some particular CAT(0) spaces [15, 16, 19].

This paper is about algorithms for finite CAT(0) polyhedral complexes, which we will call “CAT(0) complexes” from now on. We are primarily interested in the algorithmic properties of CAT(0) complexes because of their applications, particularly to computational evolutionary biology. The (moduli) space of all phylogenetic (evolutionary) trees with  $n$  leaves can be modelled as a CAT(0) cube complex with a single vertex [7], and being able to compute convex hulls in this space would give a method for computing confidence intervals for sets of trees (see Section 2.3 for more details). A second application of CAT(0) cube complexes is to reconfigurable systems [22], a large family of systems which change according to some local rules, e.g. robotic motion planning, the motion of non-colliding particles in a graph, and phylogenetic tree mutation, etc. In many reconfigurable systems, the parameter space of all possible positions of the system can be seen as a CAT(0) cube complex [22].

In this paper we study the shortest path problem and the convex hull problem in 2D CAT(0) complexes formed by triangles or rectangles. We give an algorithm to solve the single-source shortest path problem in 2D CAT(0) complexes. Given a 2D CAT(0) complex of  $n$  triangles and a source point  $s$ , our algorithm uses  $O(n^2)$  preprocessing time and  $O(n)$  storage, and finds the shortest path from  $s$  to any query point  $t$  in time proportional to the number of triangles traversed by the path. This generalizes and improves two previous results: an algorithm by Maftuleac [37] for the case of *planar* 2D CAT(0) complexes, where every edge is in at most two faces; and an algorithm by Chepoi and Maftuleac [17] for the case of 2D CAT(0) rectangular complexes.

The problem of finding the convex hull of a set of points in a 2D CAT(0) complex is significantly more challenging. For any set of points  $P$  we define the *convex hull* to be the minimal set containing  $P$  that is closed under taking the shortest path between any two points in the set. We show that convex hulls in 2D CAT(0) complexes fail to satisfy some of the properties we take for granted in Euclidean spaces. Our main result is a polynomial time algorithm to find the convex hull of a finite set of points in a 2D CAT(0) complex with a single vertex. In general, for any CAT(0) complex, the convex hull of a set of points is the union of a convex set in each cell of the complex. For the case of 2D CAT(0) complexes, these convex sets are polygons. For the special case when there is a single vertex, we show how to find these polygons using linear programming.

The rest of the paper is organized as follows. Section 2 contains further background on the problem, including existing algorithmic results for CAT(0) polyhedral complexes and applications to phylogenetics. Section 3 reviews the relevant mathematics and tree space notation. Section 4 gives our results for convex hulls, and Section 5 gives our results for shortest paths in CAT(0) polyhedral complexes. Finally we give our conclusions in Section 6.

## 2 Background

In this section we describe background work on shortest path and convex hull algorithms, and discuss the application of our work to phylogenetic trees.

One of the most basic CAT(0) spaces is the interior of any simple polygon in the plane. This can be viewed as a 2D CAT(0) complex once the polygon is triangulated. The fact that geodesic paths are unique is at the heart of efficient algorithms for shortest paths and related problems. On the other hand, generalizing a polygon to a polygonal domain (a polygon with holes) or a polyhedral terrain yields spaces that are not CAT(0), since geodesic paths are no longer unique. This helps explain why shortest path and convex hull problems are more difficult in these more general settings.

### 2.1 Shortest Paths

The shortest path problem is a fundamental algorithmic problem with many applications, both in discrete settings like graphs and networks (see, e.g., [1]) as well as in geometric settings like polygons, polyhedral surfaces, or 3-dimensional space with obstacles (see, e.g., Mitchell [39]).

All variants of the shortest path problem can be solved efficiently for a polygon once it is triangulated, and triangulation can be done in linear time with Chazelle’s algorithm [12]. The shortest path (the unique geodesic) between two given points can be found in linear time [34]. For query versions, linear space and linear preprocessing time allow us to answer single-source queries [24, 27], and more general all-pairs queries [25], where answering a query means returning the distance in logarithmic time, and the actual path in time proportional to its number of edges.

By contrast, in a polygonal domain, where geodesic paths are no longer unique, the best shortest path algorithm uses a continuous-Dijkstra approach in which paths are explored by order of distance. For a polygonal domain of  $n$  vertices, this method takes  $O(n \log n)$  [preprocessing] time [28] (see the survey by Mitchell [39]). For a polyhedral terrain the continuous-Dijkstra approach gives  $O(n^2 \log n)$  time [40], and the best-known run-time of  $O(n^2)$  is achieved by Chen and Han’s algorithm [14] that uses a breadth-first-search approach.

There are no shortest path algorithms for the general setting of CAT(0) polyhedral complexes, although there are some for certain specializations. For *planar* 2D CAT(0) complexes, where every edge is in at most two faces, Maftuleac [37] gave a Dijkstra-like algorithm for the single-source shortest path query problem, with preprocessing time  $O(n^2 \log n)$ , space  $O(n^2)$  and query time proportional to the size of the output path.

There are also some partial results on finding shortest paths when we restrict the CAT(0) polyhedral complex to be composed of cubes or rectangles. The space of phylogenetic trees mentioned in the introduction is a CAT(0) cube complex. For these “tree spaces,” Owen and Provan [43] gave an algorithm to compute shortest paths (geodesics) with a running time of  $O(m^4)$ , where  $m$  is the dimension of the maximal cubes. The algorithm is much faster in practice for realistic trees. The result was extended to a polynomial time algorithm for computing geodesics in any *orthant space* [38], where an *orthant space* is a CAT(0) cube

complex with a single vertex. The algorithm for tree space was also adapted by Ardila et al. [2] to give a finite algorithm that computes the shortest path between two points in a general CAT(0) cube complex, however this algorithm is likely not polynomial time. Finally, Chepoi and Maftuleac [17] used different methods to give a polynomial time algorithm for all-pair shortest path queries in any 2D CAT(0) rectangular complex, with preprocessing time  $O(n^2)$ , space  $O(n^2)$ , and query time larger in general than the size of the output path.

## 2.2 Convex Hulls

The problem of computing the convex hull of a set of points is fundamental to geometric computing, especially because of the connection to Voronoi diagrams and Delaunay triangulations [35].

The convex hull of a set of points in the plane can be found in provably optimal time  $O(n \log h)$  where  $n$  is the number of points and  $h$  is the number of points on the convex hull. The first such algorithm was developed by Kirkpatrick and Seidel [33] and a simpler algorithm was given by Chan [11]. An optimal algorithm for computing convex hulls in higher dimension  $d$  in time  $O(n^{\lfloor \frac{d}{2} \rfloor})$  was given by Chazelle [13]. See the survey by Seidel [45].

A simple polygon, triangulated by chords, is the most basic example of a 2D CAT(0) complex. In this setting, the convex hull of a set of points  $P$  (i.e. the smallest set containing  $P$  and closed under taking geodesics) is referred to as the *relative* (or *geodesic*) convex hull. Toussaint gave an  $O(n \log n)$  time algorithm to compute the relative convex hull of a set of points in a simple polygon [46], and studied properties of such convex hulls [47]. Ishaque and Tóth [30] considered the case of line segments that separate the plane into simply connected regions (thus forming a CAT(0) space) and gave an semi-dynamic algorithm to maintain the convex hull of a set of points as line segments are added and points are deleted.

Moving beyond polygons to polygonal domains or terrains, geodesic paths are no longer unique, so there is no single natural definition of convex hull (one could take the closure under geodesic paths, or the closure under shortest paths). We are unaware of algorithmic work on these variants.

However, in a polyhedral surface with unique geodesics—that is, in a planar 2D CAT(0) complex—the convex hull is well defined, and Maftuleac [37] gave an algorithm to compute the convex hull of a set of points in  $O(n^2 \log n)$  time, where  $n$  is the number of vertices in the complex plus the number of points in the set.

In all the above cases the boundary of the convex hull is composed of segments of shortest paths between the given points, which—as we shall see in Section 4.1—is not true in our setting of 2D CAT(0) complexes.

Beyond polyhedral complexes, convex hulls become much more complicated. Indeed it is still an open question if the convex hull of 3 points on a general Riemannian manifold of dimension 3 or higher is closed [6, Note 6.1.3.1]. Bowditch [9] and Borbély [8] give some results for convex hulls on manifolds of pinched negative curvature, but our complexes need not be manifolds. In the space of positive definite matrices, which is a CAT(0) Riemannian manifold, Fletcher et al. [21] give an algorithm to compute generalized convex hulls using horoballs, which are generalized half-spaces. Lin et al. [36] look at convex hulls of three points

in a CAT(0) cubical complex that generalizes the space of phylogenetic trees. They show that for  $d \leq 400$ , these triangles have dimension at least  $5d/6$ . Bridson and Haefliger [10, Proposition II.2.9] give conditions for when the convex hull of three points in a CAT(0) space is “flat”, or 2-dimensional. Finally, for a survey of convexity results in complete CAT(0) (aka Hadamard) spaces, of which the space of phylogenetic trees is one, see [4].

## 2.3 Application to phylogenetic trees

While this paper will look at arbitrary 2D complexes with non-positive curvature, our work is motivated by a particular complex with non-positive curvature, namely the space of phylogenetic trees introduced by Billera, Holmes, and Vogtmann [7], called the *BHV tree space*. This space is a complex of Euclidean orthants (the higher dimensional version of quadrants and octants), in which each point in the space represents a evolutionary or phylogenetic tree. Phylogenetic trees represent the evolutionary history of a set of organisms and are ubiquitous in biology.

One area of active phylogenetics research is how to statistically analyze sets of phylogenetic trees on the same, or roughly the same, set of species. Such sets can arise in various ways: from sampling a known distribution of trees, described mathematically, such as the Yule process [49]; from tree inference programs, such as the posterior distribution returned by performing Bayesian inference [44] or the bootstrap trees from conducting a maximum likelihood search [20]; or from improvements in genetic sequencing technologies that lead to large sets of gene trees, each of which represents the evolutionary of a single gene, as opposed to the species’ evolutionary history as a whole. Traditionally, most of the research in this area focused on summarizing the set of trees, although recent work has included computing variance [3, 38] and principal components [42].

It is an open question to find a good way to compute confidence regions for a set of phylogenetic trees. While work has been done on proving a central limit theorem for the BHV tree space [5], even the equivalent of a Gaussian distribution is not fully known on the BHV tree space, and thus this approach can not yet be used to compute confidence regions. Thus we must assume that the underlying distribution is unknown. In [29], Holmes proposes applying the approach of Tukey [48] for Euclidean space to the BHV tree space, namely peeling convex hulls. The convex hull is the minimum set that contains all the data points, as well as all geodesics between points in the convex hull. By peeling convex hulls, we mean to compute the convex hull for the data set, and then remove all data points that lie on the convex hull. This can then be repeated. To get the 95% confidence region, for example, one would remove successive convex hulls until only 95% of the original data points remain.

If we keep peeling convex hulls until a single point remains, we have the univariate median of Tukey [48]. This could also be a useful one-dimensional summary statistic for a set of trees. Many of the most-used tree summary statistics have a tendency to yield a degenerate or non-binary tree, which is a tree in which some of the ancestor relationships are undefined. This is considered a problem by biologists, but the univariate median tree found by peeling convex hulls would be guaranteed to be binary if all trees in the data set are.

Currently, these methods cannot be used, because it is not known how to compute convex

hulls in BHV tree space. We show several examples of how Euclidean intuition and properties for convex hulls do not carry over to convex hulls in the BHV tree space. Our algorithm to find convex hulls applies to the space of trees with five leaves which is described in more detail in Section 3.1.

### 3 Preliminaries

A metric space  $(X, d)$  is *geodesic* if every two points  $x, y \in X$  are connected by a locally shortest or *geodesic* path. A geodesic metric space  $X$  is *CAT(0)* if its triangles satisfy the following CAT(0) inequality. For any triangle  $ABC$  in  $X$  with geodesic segments for its sides, construct a *comparison triangle*  $A'B'C'$  in the Euclidean plane such that  $d(A, B) = d(A'B')$ ,  $d(A, C) = d(A'C')$ , and  $d(B, C) = d(B'C')$ . Let  $Y$  be a point on the geodesic between  $B$  and  $C$ , and let  $Y'$  be a *comparison point* on the line between  $B'$  and  $C'$  such that  $d(B, Y) = d(B'Y')$ . Then triangle  $ABC$  satisfies the CAT(0) inequality if  $d(Y, A) \leq d(Y'A')$ . Intuitively, this corresponds to all triangles in  $X$  being at least as skinny as the corresponding triangle in Euclidean space (Figure 1).

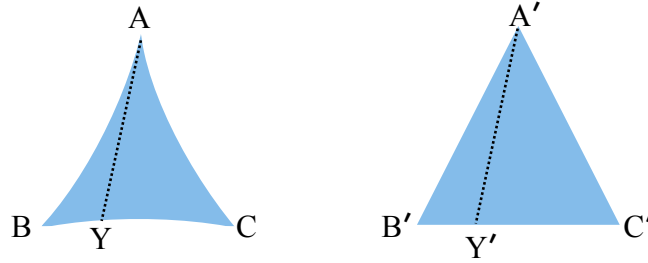


Figure 1: The triangle on the left represents a triangle in a CAT(0) space, with its corresponding comparison triangle in Euclidean space on the right.

A *polyhedral complex* is a set of convex polyhedra (“cells”) glued together by isometries along their faces. In this paper we only consider finite polyhedral complexes. When all of the cells are cubes, then this is called a *cube*, or *cubical complex*. The length of a path between two points in a polyhedral complex is the sum of the Euclidean lengths of the pieces of the path in each cell of the complex. The *distance* between two points is defined as the length of the shortest path between them.

We will consider polyhedral complexes that are CAT(0). The cells are 2D (planar) convex polygons. These can always be triangulated, so the general setting is when the cells are triangles. We call this a *2D CAT(0) complex*. Sometimes we will consider a complex in which all the cells are rectangles, either bounded or unbounded. We call this a *2D CAT(0)*

*rectangular complex*. In general we allow the space to have boundary (i.e., an edge that is incident to only one cell).

For any vertex  $v$  of a 2D complex, we define the *link graph*,  $G_v$  as follows. The vertices of  $G_v$  correspond to the edges incident to  $v$  in the complex. The edges of  $G_v$  correspond to the cells incident to  $v$  in the complex: if  $r$  and  $s$  are edges of cell  $C$  with  $r$  and  $s$  incident to  $v$ , then we add an edge between vertices  $r$  and  $s$  in  $G_v$  with weight equal to the angle between  $r$  and  $s$  in  $C$ . Every point  $p \neq v$  in cell  $C$  can be mapped to a point on edge  $(r, s)$  in  $G_v$ : if the angle between  $vr$  and  $vp$  in  $C$  is  $\alpha$  then  $p$  corresponds to the point along edge  $(r, s)$  that is distance  $\alpha$  from  $r$ . We use the same notation for a point of  $C$  and the corresponding point in the link graph when the meaning is clear from the context.

When we have a 2D polyhedral complex, there is also an alternative condition for determining whether it is CAT(0).

**Theorem 1** ([10, Theorem II.5.4 and Lemma II.5.6]). *A 2D polyhedral complex  $\mathcal{K}$  is CAT(0) if and only if it is simply connected and for every vertex  $v \in \mathcal{K}$ , every cycle in the link graph  $G_v$  has length at least  $2\pi$ .*

Some of our results are only for the case where the complex has a single vertex  $O$ , which we call the *origin*. We will call such a complex a *single-vertex complex*. In a 2D single-vertex complex every cell is a *cone* formed by two edges incident to  $O$  with angle at most  $\pi$  between them. There is a single link graph  $G_O$ . Every point of the complex except  $O$  corresponds to a point of  $G_O$ , and every point of  $G_O$  corresponds to a ray of points in the complex.

### 3.1 BHV Tree Space

The results in this paper are for 2D CAT(0) complexes. As mentioned in Section 2.3 one application is to tree spaces. In this section we describe the BHV tree space,  $\mathcal{T}_5$ , that is a 2D CAT(0) complex. The tree space  $\mathcal{T}_5$  contains all unrooted leaf-labelled, edge-weighted phylogenetic trees with 5 leaves (equivalently all such *rooted* trees with 4 leaves). For a description of the general space with more than 5 leaves, see [7]. A *phylogenetic tree* is a tree in which each interior vertex has degree  $\geq 3$  and there is a one-to-one labelling between the leaves (degree 1 vertices) and some set of labels  $\mathcal{L}$ . For this paper, we assume  $\mathcal{L} = \{1, 2, 3, 4, 5\}$ . These trees also have a positive weight or length on each interior edge.

A *split* is a partition of the leaf-set  $\mathcal{L}$  into two parts  $L_1 \cup L_2 = \mathcal{L}$  such  $|L_i| \geq 2$  for  $i = 1, 2$ . We write a split as  $L_1|L_2$ . Each edge in a phylogenetic tree corresponds to a unique split, where the two parts are the sets of leaves in the two subtrees formed by removing that edge from the tree. Trees with five leaves contain two interior edges, and hence two splits. There are 10 possible splits, and they can be combined to form 15 different tree shapes. The *shape* of a tree defines which species are most closely related, and is given by the set of interior edges or splits in that tree. (Figure 2).

Each of the 15 possible tree shapes corresponds to a Euclidean quadrant in  $\mathcal{T}_5$ . The two axes of the quadrant are labelled by the two splits in the tree shape. A point in the quadrant corresponds to the tree with that tree shape whose interior edges have the lengths given by the coordinates. We identify axes labelled by the same split, so that if two quadrants both

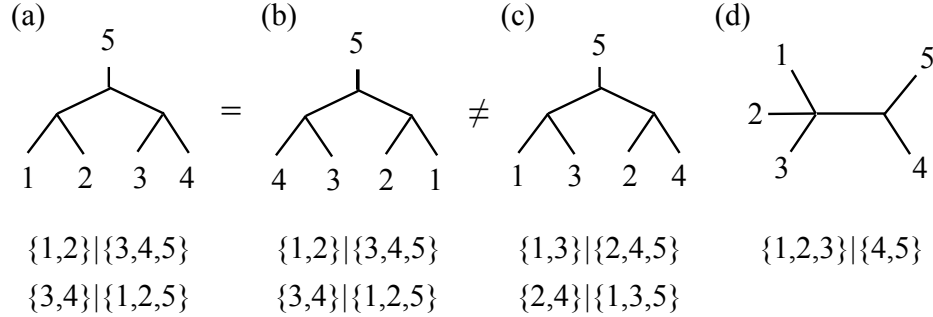


Figure 2: Several tree shapes with their constituent splits listed below them. Tree (a) and tree (b) have the same tree shape, which does not depend on the planar embedding of the tree. Tree (c) has different splits and hence a different tree shape from trees (a) and (b). Tree (d) is a non-binary tree shape.

contain an axis labelled by the same split, then they are glued together along that shared axis (see Figure 3).

The *BHV distance* is the length of the shortest path, or geodesic, between the two trees (Figure 3). Billera et al. [7] proved that this tree space is a CAT(0) cube complex, which implies that there is a unique geodesic between any two trees in the tree space.

To understand how the 15 quadrants in  $\mathcal{T}_5$  are connected, consider the link graph of the origin, which is shown in Figure 4 and is the Petersen graph. The Petersen graph has multiple overlapping 5-cycles, one of which corresponds to the 5 quadrants in Figure 3. Also note that each vertex in the link graph of the origin is adjacent to three edges. This corresponds to each axis lying in three quadrants in  $\mathcal{T}_5$ .

Note that this example illustrates that the link graph of even a CAT(0) rectangular complex with a single vertex need not be planar.

## 4 Convex Hulls

Let  $P$  be a finite set of points in a CAT(0) complex  $\mathcal{K}$ . Recall from Section 1 that the convex hull of  $P$  is defined to be the minimal set containing  $P$  that is closed under taking the shortest path between any two points in the set. Let  $\text{CH}(P)$  denote the convex hull of  $P$  in  $\mathcal{K}$ . For algorithmic purposes, there are several ways to specify  $\text{CH}(P)$ . One possibility is to specify the intersection of  $\text{CH}(P)$  with each cell of the complex. In the case of 2D CAT(0) complexes, each such set is a convex polygon, which can be given by its vertices. Our algorithm will do this. However, we note that there is another way to specify  $\text{CH}(P)$ , which might be easier but would still suffice for many applications, and that is to give an algorithm to decide if a given query point of  $\mathcal{K}$  is inside  $\text{CH}(P)$ .

Convex hulls in CAT(0) complexes are something of a mystery. It is not known, for example, whether they are closed sets [6, Note 6.1.3.1]. We begin in subsection 4.1 by giving some examples to show that various properties of Euclidean convex hulls fail in CAT(0)



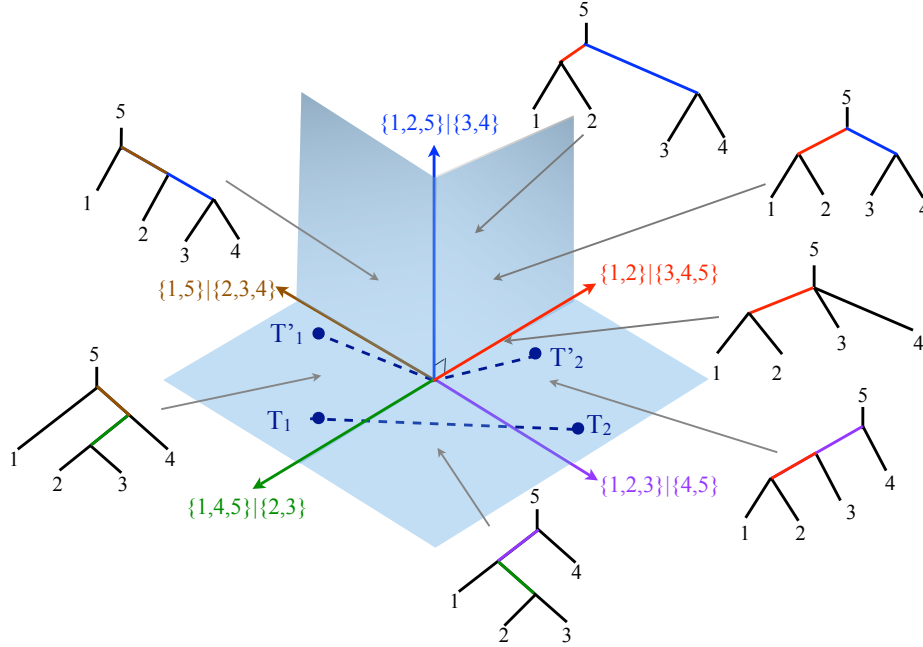


Figure 3: Five quadrants in  $\mathcal{T}_5$ . The upper right quadrant illustrates how trees with the same tree shape but different edge lengths lie at different coordinates in the quadrant. The dashed lines represent geodesics between two pairs of trees where  $T_i$  and  $T'_i$  have the same tree shape but different edges lengths. The geodesic  $T'_1$  to  $T'_2$  passes through the origin, while the geodesic  $T_1$  to  $T_2$  passes through an intermediate quadrant.

complexes. After that we give our main result, a polynomial time algorithm (using linear programming) to find convex hulls in any 2D CAT(0) complex with a single vertex  $O$ . This algorithm implies that the convex hull is closed in the case of 2D CAT(0) complexes. The idea of our algorithm is to first use the link graph to test if point  $O$  is in the convex hull and to identify the edges of the complex that intersect the convex hull at points other than  $O$ . Then we formulate the exact computation of the convex hull as a linear program whose variables represent the boundary points of the convex hull on the edges of the complex.

#### 4.1 Counterexamples for Convex Hulls in CAT(0) complexes

In this section we give examples to show that the following properties of the convex hull of a set of points  $P$  in Euclidean space do not carry over to CAT(0) complexes.

1. Any point on the boundary of the convex hull is on a shortest path between two points of  $P$ .
2. In any dimensional space, the convex hull of three points is 2-dimensional.
3. Any point inside the convex hull can be written as a convex combination of points of  $P$ .

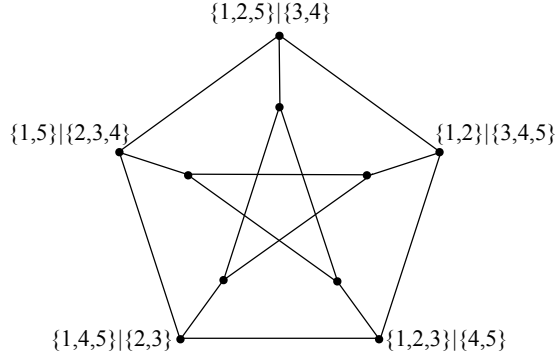


Figure 4: The Petersen graph, which is the link graph of the origin of  $\mathcal{T}_5$ . The graph edges correspond to tree shapes, and the graph vertices correspond to splits. The 5 quadrants in Figure 3 correspond to the outer 5-cycle in the Petersen graph.

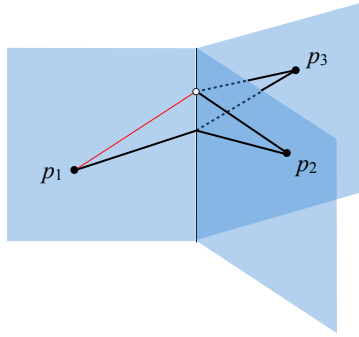


Figure 5: The shortest paths between  $p_1, p_2, p_3$  (shown in black) do not determine the convex hull because the thin red line is on the boundary of the convex hull but not on any of the shortest paths.

Our first example, shown in Figure 5, has three cells sharing an edge. Set  $P$  contains one point in each cell. The three shortest paths between pairs of points in  $P$  do not determine the convex hull. This shows that property 1 fails.

Furthermore, the example in Figure 6 shows that even in a single-vertex 2D CAT(0) rectangular complex, the convex hull of a set of points  $P$  can contain a point in a quadrant that is not entered by any shortest path between points of  $P$ .

The example in Figure 7 shows that the convex hull of three points in a 3D CAT(0) complex may contain a 3D ball. This shows that property 2 fails.

Property 3 must be expressed more carefully for CAT(0) complexes because it is not clear what a convex combination of a set of points means except when the set has two points. If  $p$  and  $q$  are two points in a CAT(0) complex, then the points along the shortest path from  $p$  to  $q$  can be parameterized as  $(1 - t)p + tq$  for  $t \in [0, 1]$ . Based on the definition of the convex hull, any point in the convex hull of a set of points  $P$  can be represented as a rooted binary tree with leaves labelled by points in  $P$  (with repetition allowed) and with the two

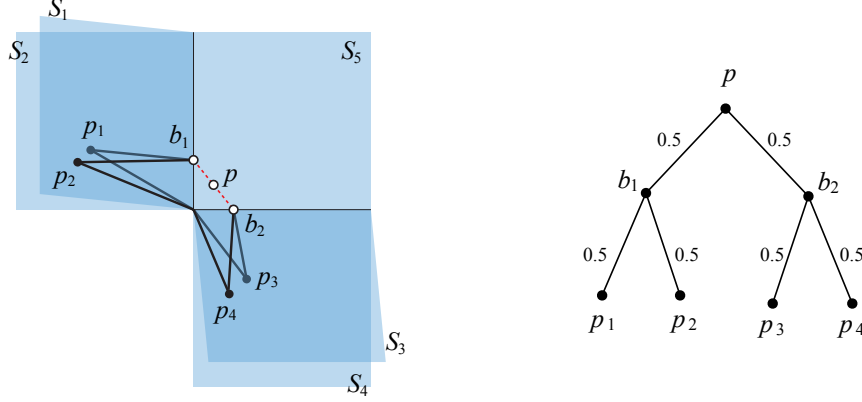


Figure 6: (left) A 2D CAT(0) space consisting of 5 quadrants. Quadrants  $S_1, S_2, S_5$  share a vertical edge, and quadrants  $S_3, S_4, S_5$  share a horizontal edge. Point  $p_i, i = 1, 2, 3, 4$ , lies in quadrant  $S_i$ . The convex hull of  $p_1, p_2, p_3, p_4$  contains points—in particular  $p$  and the dashed red line—in a quadrant,  $S_5$ , that is not entered by any shortest path between points of  $P$  (shown as black lines). Note that 4 of the 6 shortest path between points of  $P$  go through the origin. (right) The tree representation of point  $p$  in terms of  $P$ .

child edges of each internal node  $v$  labelled by two numbers  $(1 - t_v)$  and  $t_v$  for  $t_v \in [0, 1]$ , meaning that the point associated with  $v$  is this combination of the points represented by the child nodes. For example, see Figure 6.

One might hope that every point in the convex hull can be represented by a binary tree whose leaves are labelled by distinct elements of  $P$ , but this is false for the example in Figure 7.

Furthermore, this property may even fail for a 2D CAT(0) complex as we prove below for the example in Figure 8:

**Lemma 1.** *For the 2D CAT(0) complex shown in Figure 8, the point  $p$  cannot be represented by a binary tree with distinct leaves from  $\{p_1, p_2, p_3, p_4\}$ .*

*Proof.* From the link graph (shown in Figure 8(b)), the angle between  $p_3$  and  $p_4$  is  $180^\circ$  so the geodesic between them goes through the origin. Similarly, the geodesics between the following pairs also go through the origin:  $p_3$  and  $p_2$ ;  $p_3$  and  $p_1$ ;  $p_2$  and  $p_4$ . The only pairs with angles less than  $180^\circ$  are  $p_1, p_2$ , and  $p_1, p_4$ . The geodesic from  $p_1$  to  $p_2$  crosses axis 3 at point  $a$ . The geodesic from  $p_1$  to  $p_4$  crosses axis 5 at point  $c$ . Because  $p_1$  is closer to axis 2, point  $c$  is closer to the origin than point  $a$  (see Figure 8(d)). The geodesic paths from  $p_3$  to both  $a$  and  $c$  cross axis 4 and thus can be used to construct points in the cell bounded by axes 4 and 5 (where  $p$  lies). However, as shown in Figure 8(e), the geodesic path from  $p_3$  to  $a$  crosses axis 4 further from the origin at point  $b$ , and therefore point  $p$  can only be constructed using points  $a$  and  $b$ , as shown by the binary tree in Figure 8(b). Therefore  $p$  can only be represented by a binary tree that repeats the leaf  $p_1$ .  $\square$

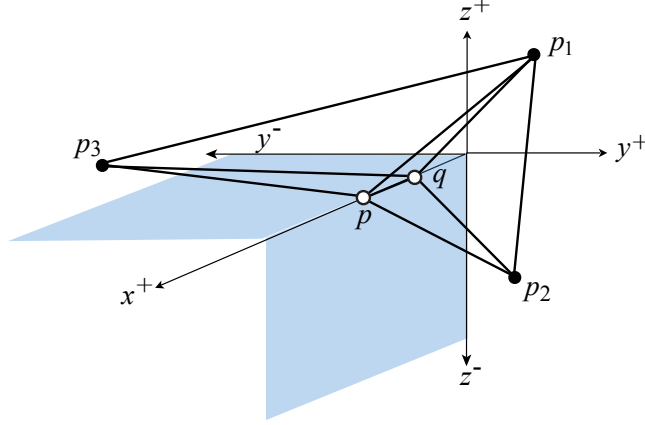


Figure 7: The convex hull of the three points  $p_1, p_2, p_3$  in this 3D CAT(0) complex contains a 3D ball. Point  $p_1$  lies in the  $x^+y^+z^+$  octant,  $p_2$  in the  $x^+y^+z^-$  octant, and  $p_3$  in the  $x^+y^-z^+$  octant. The  $x^+y^-z^-$  octant is missing. Point  $p$  is where the shortest path from  $p_2$  to  $p_3$  intersects the  $x^+$  axis, and point  $q$  is where the triangle  $p_1p_2p_3$  is pierced by the  $x^+$  axis. The convex hull of  $P$  consists of the union of two simplices  $p_1p_3pq$  and  $p_1p_2pq$ .

## 4.2 Convex Hull Algorithm for a Single-Vortex 2D CAT(0) Complex

In this section we prove our main result:

**Theorem 2.** *There is a polynomial time algorithm to find the convex hull of a finite set of points  $P$  in a 2D CAT(0) complex  $\mathcal{K}$  with a single vertex  $O$ .*

### 4.2.1 Combinatorics of the Convex Hull

In this subsection we show how to decide if  $O$  is in the convex hull and how to identify the edges of  $\mathcal{K}$  that contain points of the convex hull other than  $O$ . We will do this using the link graph  $G = G_O$ .

First consider the problem of testing whether  $O$  is in the convex hull. If  $O \in P$  we are done, so assume that  $O \notin P$ . Consider two points  $a$  and  $b$  in  $\mathcal{K}$ , distinct from  $O$ , and consider the corresponding points  $a$  and  $b$  in  $G$ . Let  $\sigma(a, b)$  be the (unique) geodesic path between  $a$  and  $b$  in the space  $\mathcal{K}$ . Let  $\sigma_G(a, b)$  be the shortest path between  $a$  and  $b$  in  $G$ . Let  $|\sigma|$  indicate the length of path  $\sigma$ . Then exactly one of the following two things holds:

- $|\sigma_G(a, b)| \geq \pi$  and  $\sigma(a, b)$  goes through  $O$ ,
- $|\sigma_G(a, b)| < \pi$  and  $\sigma(a, b)$  maps to  $\sigma_G(a, b)$  and does not go through  $O$ .

Now, since  $O$  is in  $\text{CH}(P)$  if and only if there is a path between two points in  $\text{CH}(P) - O$  that goes through  $O$ , we have:

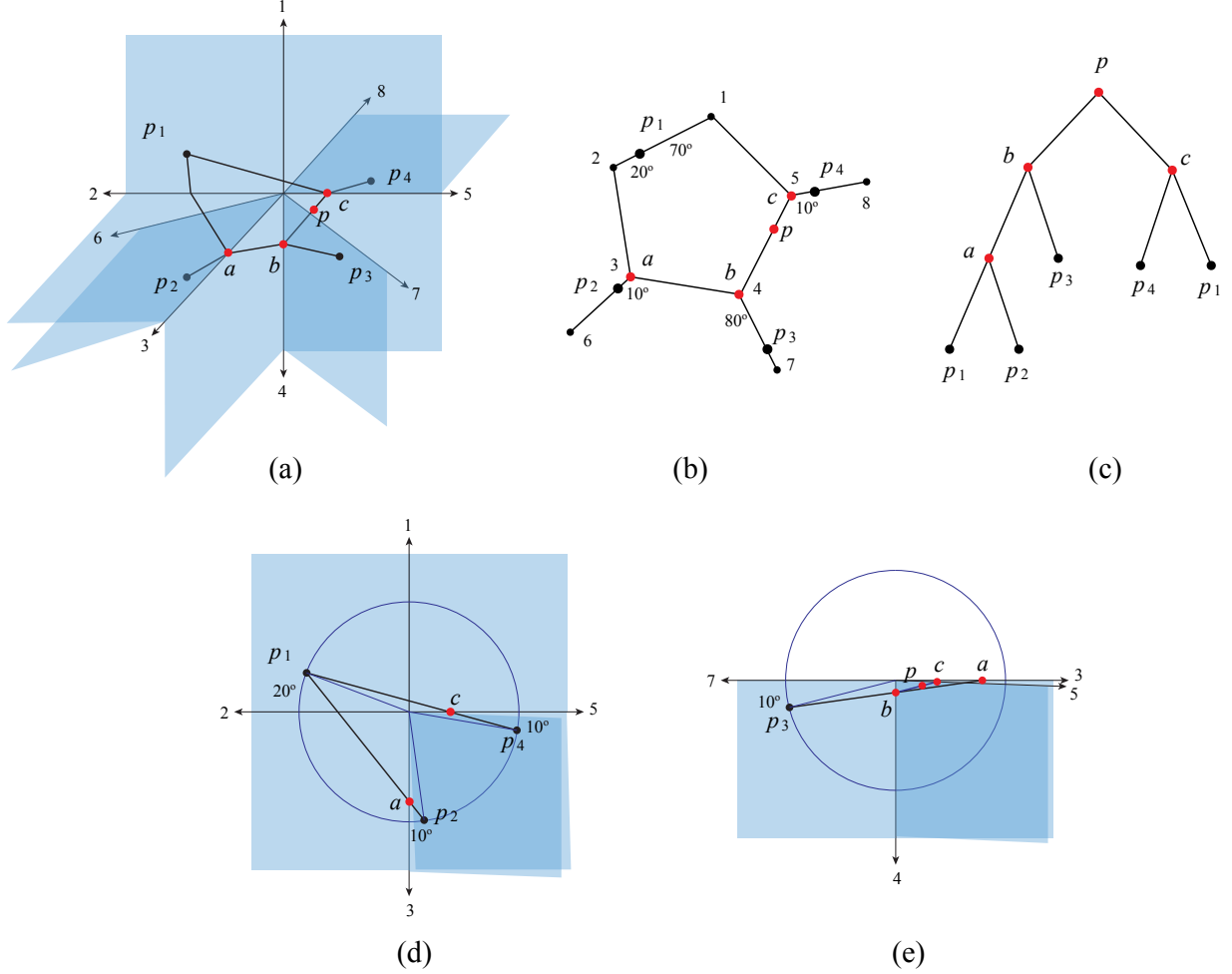


Figure 8: An example of a 2D CAT(0) complex where point  $p$  in  $\text{CH}(\{p_1, p_2, p_3, p_4\})$  cannot be represented as a binary tree with distinct leaves. Points  $p_1, p_2, p_3, p_4$  are all distance 1 from the origin, with angles as specified in the link graph. (a) the complex (not to scale); (b) the link graph; (c) the binary tree representing  $p$ ; (d) construction of points  $a$  and  $c$ ; (e) construction of points  $b$  and  $p$ .

**Observation 1.**  $O$  is in  $\text{CH}(P)$  if and only if there are two points  $a$  and  $b$  in  $\text{CH}(P) - O$  such that the distance between  $a$  and  $b$  in the link graph is at least  $\pi$ .

We test if  $O$  is in  $\text{CH}(P)$  as follows. If there are two points  $p, q \in P$  whose distance in the link graph is at least  $\pi$ , then  $O$  is in  $\text{CH}(P)$ . Otherwise, let  $G[P]$  be the subset of the link graph that is the union of all shortest paths  $\sigma_G(p, q)$ ,  $p, q \in P$ . Note that  $G[P]$  is not a subgraph of  $G$  in the usual sense because in general it includes portions of edges. Every point of  $G[P]$  is the image of some point in  $\text{CH}(P)$ . By the following lemma, it suffices to test if  $G[P]$  has a cycle.

**Lemma 2.** *Suppose that no path between two points of  $P$  goes through  $O$ . Then  $O \in \text{CH}(P)$  if and only if  $G[P]$  contains a cycle.*

*Proof.* Suppose  $G[P]$  contains a cycle. Because the space is  $\text{CAT}(0)$ , the cycle has length at least  $2\pi$ , so it must contain two points  $a, b$  whose minimum distance in the cycle is  $\pi$ . Then the length of the shortest path between  $a$  and  $b$  in the link graph is  $\pi$  (otherwise we would have a cycle of length less than  $\pi$ ). By Observation 1,  $O$  is in  $\text{CH}(P)$ .

For the other direction, suppose  $G[P]$  does not contain a cycle.  $G[P]$  is connected, so it must be a tree. We claim that the leaves of the tree are points of  $P$ : If  $d$  is a point of  $G[P]$  that is not in  $P$  then  $d$  is an internal point of some path  $\sigma_G(p, q)$ ,  $p, q \in P$ , so  $d$  has degree at least 2 in  $G[P]$ , so it is not a leaf.

Let  $a$  and  $b$  be points of  $G[P]$ . The path between  $a$  and  $b$  in  $G[P]$  can be extended to a path between leaves of  $G[P]$ , and, since the leaves are in  $P$ , this path has length less than  $\pi$ . Thus there is a path between  $a$  and  $b$  in  $G[P]$  of length less than  $\pi$ . This must be the shortest path between  $a$  and  $b$  in  $G$ . Thus,  $G[P]$  is closed under taking shortest paths. We will never get two points at distance  $\pi$  or more. Therefore  $O$  is not in the convex hull.  $\square$

The algorithm to test if  $O$  is in  $\text{CH}(P)$  has a straight-forward implementation that runs in time  $O(m(n + m))$  where  $n$  is the number of cells in  $\mathcal{K}$  and  $m$  is the size of  $P$ . For each point  $p \in P$ , we do a depth-first search in the link graph to find paths to all the points of  $P$  within distance  $\pi$  of  $p$ . Note that a search to distance  $\pi$  will not find any cycles in the link graph, and therefore finds shortest paths from  $p$ . If some point  $q \in P$  is not reached then we know that  $O$  is in  $\text{CH}(P)$ . Otherwise, we construct  $G[P]$  as the union of all these depth-first search trees, and test if  $G[P]$  contains a cycle. Each depth-first search takes time  $O(n + m)$  so the total time is  $O(m(n + m))$ . Constructing and exploring  $G[P]$  takes linear time.

We now show how to identify the edges of the complex  $\mathcal{K}$  that contain points of  $\text{CH}(P) - O$ . Equivalently, we will identify the vertices of the link graph that correspond to points in the convex hull. Our method applies whether or not  $O$  is inside the convex hull.

We will build up a set  $S$  of points and vertices in the link graph. Initially  $S$  will just be the input set of points  $P$ , and at the end of the algorithm,  $S$  will also contain all vertices of the link graph that correspond to points in the convex hull. We will also keep a subset  $F$  of  $S$  that represents the “frontier” that we still need to explore from. Initially  $F = S = P$ .

The general step is to remove one element  $v$  from  $F$ . We then explore the part of the link graph within distance  $\pi$  from  $v$ . This can be done by a depth-first search in  $O(n + m)$  time. As noted above, a search tree to distance  $\pi$  will find no cycles, and will therefore find shortest paths from  $v$ . We remove the part of the depth-first tree that is beyond the deepest point of  $S$  on each branch. Then for every vertex  $w$  of the link graph that is in the depth-first search tree, we check if  $w$  is already in  $S$ —if not then we add  $w$  to  $S$  and to  $F$ .

The size of  $S$  is bounded by  $n + m$  where  $n$  is the number of cells in  $\mathcal{K}$  and  $m$  is the size of  $P$ . Note that the amount of work we do for one element of  $F$  is  $O(n + m)$ . Thus the algorithm runs in time  $O((n + m)^2)$ .

The algorithm is correct because the final set  $S$  is closed under taking shortest paths of length less than  $\pi$  in the link graph.

### 4.2.2 Finding the Convex Hull

In this section we give a polynomial time algorithm to explicitly find the convex hull of a finite point set  $P$  in a 2D CAT(0) complex  $\mathcal{K}$  with a single vertex  $O$ .

Suppose first that the origin  $O$  is inside the convex hull. The case where the origin is not inside the convex hull will be dealt with later. It suffices to describe the intersection of the convex hull with each cell of the complex. Consider a cell  $C$  bounded by rays  $e$  and  $f$  incident to  $O$ . The part of the convex hull inside  $C$  is a convex polygon determined by its vertices which consist of: point  $O$ ; the points of  $P$  inside  $C$ ; and two points  $x_e$  and  $x_f$  on edges  $e$  and  $f$ , respectively, that are on the boundary of the convex hull. Note that we do not make any assumption about whether  $x_e$  and  $x_f$  are in the convex hull, because we are not making any assumption about whether the convex hull is open or closed.

Let  $B$  be the set of edges of the complex that have points other than  $O$  inside the convex hull. These are found as described in the previous section. For each  $\ell \in B$  make a variable  $x_\ell \in \mathbb{R}$  representing the point on  $\ell$  that is on the boundary of the convex hull. Then  $x_\ell > 0$ . To “find” the convex hull, it suffices to find the values of the variables  $x_\ell$ .

There is an obvious iterative approach: Initialize  $H_0$  to be the set  $P$ . For  $i = 1, 2, \dots$ , initialize  $H_i$  to  $H_{i-1}$  and then take every pair of points from  $H_{i-1}$ , compute the shortest path  $\sigma$  between them, and add to  $H_i$  all the intersection points of  $\sigma$  with edges of the complex. (When two points lie on the same edge, we can discard the one closer to  $O$ .) In order for this to be an efficient algorithm we would need a bound on the number of iterations, but we do not even have a finite bound, although we make the following conjecture:

**Conjecture 1.**  $H_k = H_{k+1}$  for some polynomially bounded  $k$ .

Rather than using iteration we will find the values for  $x_\ell$  using linear programming.

Our inequalities will be determined by pairs of elements from the set  $L = P \cup B$ . Notation will be eased by viewing elements of  $P$  and of  $B$  uniformly, which we can do by constructing an edge  $e_p$  through each point of  $p \in P$  (subdividing its cell) and associating  $p$  with the variable  $x_{e_p}$  which has a known constant value. Then for any two elements  $e$  and  $f$  of  $L$ , such that the angle between  $e$  and  $f$  is  $< \pi$ , consider the shortest path  $\sigma$  between the corresponding points. We will add a constraint for each edge  $\ell$  of  $\mathcal{K}$  crossed by  $\sigma$ , expressing the fact that the convex hull includes the point where  $\sigma$  crosses  $\ell$ . The constraint has the form  $x_\ell \geq t$  where  $t$  is the point where  $\sigma$  crosses  $\ell$ . (More precisely,  $t$  is the distance from  $O$  to the crossing point.) We can express  $t$  in terms of known quantities. The set-up is illustrated in Figure 9. Note that there may be several polyhedral cells separating  $e$  and  $f$ , but we can lay them down to form a triangle.

Let  $\gamma_1$  be the angle between  $e$  and  $\ell$ , and let  $\gamma_2$  be the angle between  $\ell$  and  $f$ . Then we have:

**Claim 1.**

$$t = \frac{x_e x_f \sin(\gamma_1 + \gamma_2)}{x_e \sin \gamma_1 + x_f \sin \gamma_2}$$





Thus we have reduced the problem of finding the convex hull (when  $O$  is in the convex hull) to linear programming which can be solved in polynomial time [31, 32].

At the beginning of the algorithm we test if  $O$  is in the convex hull, and find the set  $B$  of edges of the complex that contain points of the convex hull other than  $O$ . This takes  $O((n + m)^2)$  time as discussed in the previous section. The set  $B$  has size  $O(m)$  and the set  $L$  has size  $O(n + m)$ , where  $n$  is the number of points in  $P$  and  $m$  is the number of cells in the complex. The linear program has  $O(m)$  variables. The number of inequalities is  $O(m(n + m)^2)$  since we consider each pair of elements,  $e, f$  from  $L$ , and add an inequality for each edge of the complex crossed by the shortest path from  $e$  to  $f$ . Then we rely on polynomial-time linear programming algorithms to give our claimed polynomial run-time.

We now deal with the case where the origin  $O$  is not inside the convex hull. In this case, by Lemma 2, the subgraph of the link graph corresponding to the convex hull is a tree, and it seems even more plausible that an iterative approach can be used to find the convex hull. However, we leave this as an open question, and give a linear programming approach like the one above.

Let  $B$  be the set of edges of the complex that have points other than  $O$  inside the convex hull. For each  $\ell \in B$  we will make two variables,  $x_\ell^{\min}$  and  $x_\ell^{\max}$  in  $\mathbb{R}$  representing the minimum and maximum points on  $\ell$  that are on the boundary of the convex hull. To find the convex hull, it suffices to find the values of these variables.

We want to ensure that  $x_\ell^{\max}$  is larger than any crossing point on edge  $\ell$  and that  $x_\ell^{\min}$  is smaller than any crossing point on edge  $\ell$ . Using the same notation and set-up as above with edges  $e$  and  $f$ , and using the inverse variables  $y_\ell^{\min} = \frac{1}{x_\ell^{\min}}$  and  $y_\ell^{\max} = \frac{1}{x_\ell^{\max}}$  these properties are captured by the following two inequalities:

$$\begin{aligned} y_\ell^{\max} &\leq y_f^{\max} \frac{\sin \gamma_1}{\sin(\gamma_1 + \gamma_2)} + y_e^{\max} \frac{\sin \gamma_2}{\sin(\gamma_1 + \gamma_2)} \\ y_\ell^{\min} &\geq y_f^{\min} \frac{\sin \gamma_1}{\sin(\gamma_1 + \gamma_2)} + y_e^{\min} \frac{\sin \gamma_2}{\sin(\gamma_1 + \gamma_2)} \end{aligned}$$

If we maximize the objective function  $\sum (y_\ell^{\max} - y_\ell^{\min})$  subject to the above inequalities and  $y_\ell^{\min} \geq y_\ell^{\max} \geq 0$  then, by a similar argument to the one above, this gives the convex hull of  $P$ .

Thus we have reduced the problem of finding the convex hull to linear programming. This completes the proof of Theorem 2.

## 5 Shortest Paths

This section is about the single-source shortest path problem in a 2D CAT(0) complex. The input is a 2D CAT(0) complex,  $\mathcal{K}$ , composed of  $n$  triangles, and a point  $s$  in  $\mathcal{K}$ . We will build a data structure that allows us to find, for any query point  $t$ , the shortest path from  $s$  to  $t$ , denoted  $\sigma(s, t)$ . We will achieve  $O(n^2)$  preprocessing time,  $O(n)$  storage, and query time proportional to the number of triangles and edges traversed by the path.

Typically in a shortest path problem, the difficulty is to decide which of multiple geodesic (or locally shortest) paths to the destination is shortest. This is the case, for example, for shortest paths in a planar polygon with holes, or for shortest paths on a terrain, and is a reason to use a Dijkstra-like approach that explores paths to all target points in order of distance. For shortest paths on a terrain, Chen and Han [14] provided an alternative that uses a Breadth-First-Search (BFS) combined with a clever pruning when two paths reach the same target point.

When geodesic paths are unique, however, it is enough to explore all geodesic paths, and there is no need to explore paths in order of distance or in BFS order. This is the case, for example, for shortest paths in a polygon, where the “funnel” algorithm [24, 27] achieves  $O(n)$  processing time and storage, and  $O(\log n)$  query time (plus output size to produce the actual path).

In a CAT(0) complex, geodesic paths are unique. One approach to the single source shortest path problem is to compute the whole shortest path map from  $s$ , partitioning each face into regions where all points have the same combinatorial shortest path. In a 2D CAT(0) complex the shortest path map has worst case size  $\Theta(n^2)$ , and can be computed with  $O(n^2)$  time and storage, so that the shortest path to query point  $t$  can be found in time proportional to the number of faces along the path. We do not see how to achieve linear preprocessing time as in the funnel algorithm, nor how to find the distance to a query point in logarithmic time, but we will improve the storage. We will achieve  $O(n^2)$  preprocessing time, and  $O(n)$  storage, and we will recover a shortest path to query point  $t$  in time proportional to the number of faces along the path.

The high-level idea as follows. Starting with the faces containing  $s$ , we expand to adjacent faces, constructing the *last-step shortest path map* in which two points  $p$  and  $q$  inside a face are *equivalent* if  $\sigma(s, p)$  and  $\sigma(s, q)$  enter the face on the same edge/vertex. We thus store a constant amount of information for each face. See Figure 10. We show that this information is sufficient to recover the path from  $s$  to any point  $t$  in time proportional to the number of faces on the path. This involves “unfolding” the faces along the path into the plane. The idea of storing in each face only the combinatorial information about the last step of the shortest path comes from [18].

We now fill in the details of our algorithm.

The algorithm will categorize faces according to how shortest paths enter them. Shortest paths may enter a face through: one edge (type  $E$ ); one vertex (type  $V$ ); one edge and an incident vertex (type  $EV$ ); or two edges and their common vertex (type  $EVE$ ). There are no other possibilities otherwise there would be a point in the face reached by more than one shortest path. See Figure 10. Shortest paths may reach an edge from an incident face, or from an endpoint of the edge when the edge itself lies on a shortest path. Note that different points on an edge  $e$  cannot be reached by shortest paths through different faces incident to  $e$  otherwise, by continuity, there would be a point on  $e$  reached by two geodesic paths.

The algorithm will discover how shortest paths enter each face, edge and vertex. For each face we store the *incoming* edge(s)/vertex through which shortest paths enter the face. For faces of types  $EV$  or  $EVE$  we store the one or two rays that form the boundaries of the

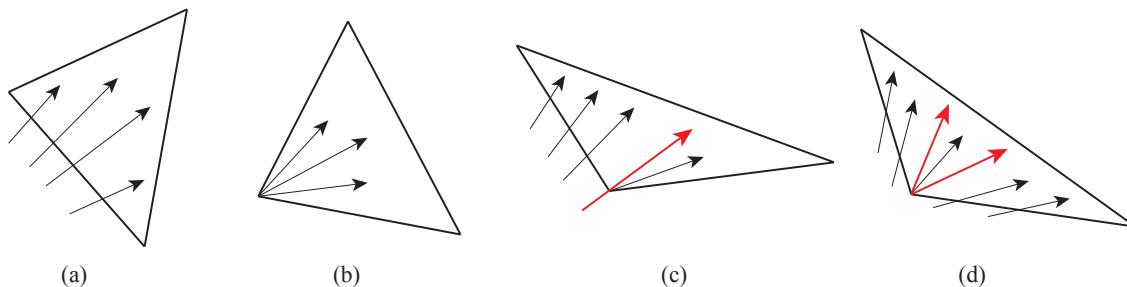


Figure 10: Shortest paths may enter a face through: (a) one edge (type  $E$ ); (b) one vertex (type  $V$ ); (c) one edge and an incident vertex (type  $EV$ ); or (d) two edges and their common vertex (type  $EVE$ ). For type  $EV$  and  $EVE$  faces we store the rays (shown in bold red) that partition the face based on the edge/vertex through which shortest paths enter.

part of the face reached by shortest paths through the vertex, as shown in Figure 10. For each edge we store the *incoming* face/vertex through which shortest paths reach the edge. For each vertex we store the *incoming* face or edge that contains the last segment of the shortest path to the vertex, and in the case of an incoming face we store the last segment of the shortest path to the vertex. In general, a ray or segment is given in local coordinates of the face in which it lies (i.e., in terms of vertices of the face). Note that the *incoming* information has constant size per face/edge/vertex, and therefore linear size overall.

At the beginning of the algorithm every face/edge/vertex is unmarked. When we have complete information about shortest paths to a face/edge/vertex then it is marked *explored*. We will have a third category for edges and vertices—an edge or vertex marked *frontier* is one that we know the shortest path to (via *incoming* information), but have not explored beyond. The general step is to take an edge or vertex out of the frontier and “explore” beyond it, moving some incident faces/edge/vertices out of the unmarked category into the frontier or explored category. The algorithm terminates when every face/edge/vertex is marked *explored*.

We now give the details of the algorithm to build the data structure for shortest path queries. The algorithm to answer shortest path queries is described later on. The two methods are entwined, because we need to answer shortest path queries in order to build the data structure.

**Initialization.** Assume that  $s$  is a vertex of the complex (if necessary, by triangulating the face containing  $s$ ). For each edge  $e = (s, v)$  incident to  $s$ , mark  $e$  as “explored” with incoming vertex  $s$  and put  $v$  into the frontier with entering ray  $sv$ . For each face  $f$  incident to  $s$ , mark  $f$  as “explored”, and as type  $V$  with incoming vertex  $s$  and put the edge of  $f$  not incident to  $s$  into the frontier with incoming face  $f$ .

**General Step.** Until the frontier is empty, take a vertex or edge out of the frontier and explore beyond it as specified in the following cases. Before we take an edge out of the frontier, there are special conditions that must be met, which we describe below.

**I. Taking a vertex  $v$  out of the frontier.** Mark  $v$  “explored”. Let  $r$  be the incoming

ray to  $v$ . Starting from point  $r$  in  $v$ 's link graph  $G_v$ , we search the link graph to identify all points within distance  $\pi$  from  $r$ . The complementary set (all points in  $G_v$  of distance  $\geq \pi$  from  $r$ ) correspond to points in  $\mathcal{K}$  that have shortest paths that go through  $v$ , and we call this set the *ruffle* of  $v$ . Note that this includes the case where  $v$  is on the boundary. See Figure 11. For each edge  $e = (v, u)$  incident to  $v$ , if  $e$  is in the ruffle then we mark  $e$  “explored” with incoming vertex  $v$  and we put  $u$  in the frontier with incoming ray  $vu$ .

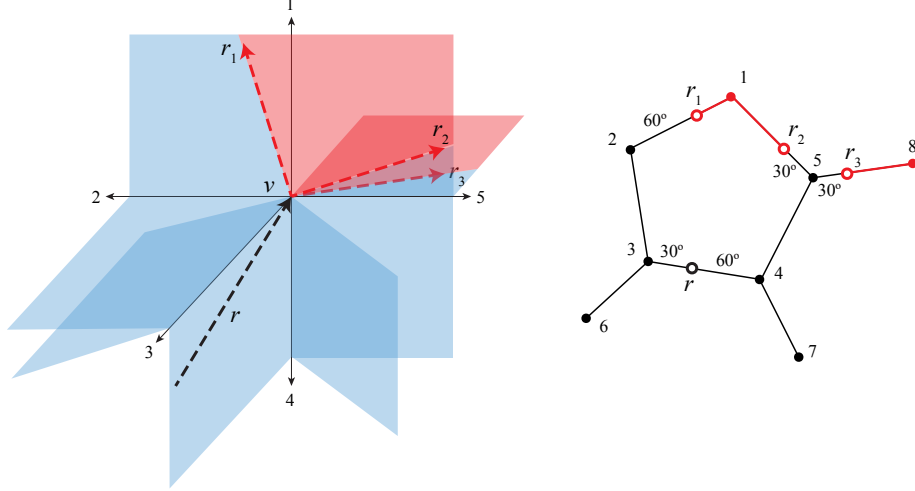


Figure 11: The ruffle (in red) of vertex  $v \in \mathcal{K}$  with respect to incoming ray  $r$ , shown in  $\mathcal{K}$  (left) and in the link graph  $G_v$  (right).

For each face  $f$  incident to  $v$  we consider several cases depending on how  $f$  intersects the ruffle of  $v$ . Let  $e = (a, b)$  be the edge of  $f$  not incident to  $v$ .

**Case 0.** No point of  $e$  is inside the ruffle. Do nothing, as no shortest paths to this face pass through  $v$ .

**Case 1.** Both  $a$  and  $b$  are inside the ruffle. Note that all of  $f$  is in the ruffle because  $f$  corresponds in the link graph  $G_v$  to an edge whose endpoints (corresponding to  $a$  and  $b$ ) are distance  $\geq \pi$  from  $r$ , so all points internal to the edge are also distance  $\geq \pi$  from  $r$ . Mark  $f$  “explored” of type  $V$  with incoming vertex  $v$ , and put  $e$  in the frontier with incoming face  $f$ .

**Case 2.** Exactly one of  $a$  or  $b$  (say  $a$ ) is inside the ruffle. Mark  $f$  of type  $VE$  with incoming vertex  $v$  and incoming edge  $(v, b)$ . A boundary ray of the ruffle goes from  $v$  to a point on the edge  $(a, b)$ . We store this ray with the face  $f$ . Note that we do not yet mark  $f$  as “explored”—we will only do that after exploring edge  $(v, b)$ .

**Case 3.** Neither  $a$  nor  $b$  is inside the ruffle but some interior point(s) of  $e$  are in the ruffle. Mark  $f$  of type  $EVE$  with incoming vertex  $v$  and incoming edges  $(v, b)$  and  $(v, a)$ . If a single point of  $e$  is inside the ruffle then exactly one ray goes from  $v$  to a point on the edge  $e$ , and otherwise two boundary rays of the ruffle go from  $v$  to points on the edge  $e$ . We store these rays with the face  $f$ . Note that we do not yet mark  $f$  as “explored”—we will only do that after exploring edges  $(v, b)$  and  $(v, a)$ .

**II. Taking an edge  $e$  out of the frontier.** We only take an edge  $e = (u, v)$  out of the frontier if both vertices  $u$  and  $v$  have already been explored. Mark  $e$  as “explored”. Let  $g$  be the incoming face for  $e$ . For each face  $f \neq g$  incident to  $e$ , let  $w$  be the third vertex of  $f$  and do the following.

**Case 1.** If  $f$  is not already marked *VE* or *EVE* then we mark  $f$  “explored” of type *E* with incoming edge  $e$ . We put the edges  $(u, w)$  and  $(v, w)$  in the frontier with incoming face  $f$ . Using the method described below, we find the shortest path from  $s$  to  $w$  and the segment  $r$  along which the shortest path reaches  $w$ . We put vertex  $w$  in the frontier with entering segment  $r$  and incoming face  $f$ .

**Case 2.** If  $f$  is marked *VE* with, say,  $v$  as an incoming vertex then we mark  $f$  “explored” and put edge  $(u, w)$  in the frontier with incoming face  $f$ . (The case when  $u$  is the incoming vertex is symmetric.)

**Case 3.** If  $f$  is marked *EVE* with, say,  $v$  as an incoming vertex then if edge  $(v, w)$  is already explored we mark  $f$  “explored” and put edge  $(u, w)$  in the frontier with incoming face  $f$ . (The case when  $u$  is the incoming vertex is symmetric.)

Correctness of the algorithm is straightforward by induction on the number of faces. The one thing worth commenting on is our condition about not removing an edge from the frontier until both its vertices have been explored. Since an edge only enters the frontier when both endpoints are in the frontier or already explored, we can always remove something from the frontier unless it is empty. When the frontier is empty, all faces, edges and vertices will be explored.

We now analyze the run time of the algorithm. Each edge/vertex enters the frontier only once. The time to process a vertex (step I) is proportional to the number of incident edges and faces, so this is linear overall. The time to process an edge (step II) is proportional to the number of incident faces times the time to recover a shortest path to a point (point  $w$  in case 1). As shown below, it takes  $O(n)$  time to recover a shortest path. Thus the total run time is  $O(n^2)$ . Storage is  $O(n)$ .

We now describe how to answer a query for the shortest path to a point  $t$ . We can do this as soon as the face/edge/vertex containing  $t$  has been explored—the algorithm need not have terminated. If  $t$  is a vertex, or a point on an edge, we can tell from the incoming information if a shortest path reaches  $t$  along an edge, say the edge from  $u$  to  $v$ . In this case, we replace  $t$  by  $u$  and recurse.

In the more general case  $t$  lies in a face, edge or vertex and we know that a shortest path reaches  $t$  through a face, say  $f$ . If  $f$  is of type *V*, we replace  $t$  by the incoming vertex of  $f$  and recurse. If  $f$  is of type *VE* or type *EVE* we locate  $t$  relative to the rays in  $f$ . From this we can tell if the shortest path to  $t$  goes through a vertex of  $f$  or not. If it does, then we replace  $t$  by that vertex and recurse.

We are left with the case where the shortest path to  $t$  enters face  $f$  through some edge, say edge  $e$ . Let  $g$  be the incoming face for edge  $e$ . We place  $f$  in the plane and attach triangle  $g$  to edge  $e$ . The placement of  $f$  is arbitrary, but then  $t$  and  $g$  are fixed. Now we enter the main loop of the algorithm (see Figure 12): If  $g$  is of type *V*, we replace  $t$  by the incoming vertex of  $g$  and recurse. If  $g$  is of type *VE* or type *EVE* we locate  $t$  relative to the

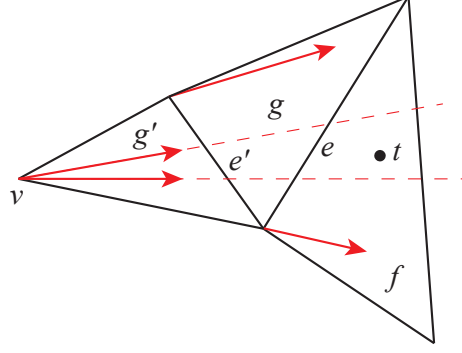


Figure 12: Finding the shortest path from  $s$  to point  $t$  in face  $f$ . In this example,  $f$  is of type  $VE$ . Testing the ray of  $f$ , we find that the shortest path to  $t$  enters from edge  $e$  which has incoming face  $g$  of type  $VE$ . Testing the rays of  $g$ , we find that the shortest path to  $t$  enters from edge  $e'$  which has incoming face  $g'$  of type  $EVE$ . Finally, testing the rays of  $g'$  we find that the shortest path to  $t$  comes from vertex  $v$ . We recursively find the shortest path to  $v$ .

rays in  $g$  (although  $t$  is not in  $g$  we just extend the rays to do the test). From this we can tell if the shortest path to  $t$  goes through a vertex of  $g$  or not. If it does, then we replace  $t$  by that vertex and recurse. Otherwise the shortest path to  $t$  enters  $g$  through an edge, and we repeat with the incoming face of that edge.

This algorithm will find the shortest path from  $s$  to  $t$  in time proportional to the number of triangles and edges on the path, which is  $O(n)$  in the worst case.

To wrap up, the whole algorithm takes time  $O(n^2)$  to preprocess the complex from  $s$ , and results in a structure of space  $O(n)$  that allows searching for a path to  $t$  in time proportional to the size of the path.

It is possible that results of Mount [41] might provide an algorithm that uses  $O(n^2)$  time,  $O(n \log n)$  space, and answers queries for the distance in  $O(\log n)$  time<sup>1</sup>. The rough idea is to store the whole shortest path map via nested trees that allow us to search all the rays entering a triangle.

## 6 Conclusions

We have given polynomial-time algorithms for computing convex hulls and shortest paths in 2D  $CAT(0)$  polyhedral complexes. The algorithm for computing convex hulls relies on linear programming, and we leave it as an open question to find a combinatorial algorithm, or prove that a simple iterative approach takes polynomial time (Conjecture 1).

We do not see how to extend our linear programming solution to higher dimensional  $CAT(0)$  complexes. In 2D, the codimension-1 boundary between maximal cells is an edge, and we only need to store one point (or two when the convex hull does not contain the

<sup>1</sup>Thanks to Stefan Langerman for this suggestion

origin) for the convex hull. In higher dimensions, this boundary has dimension 2 or greater, and it is not clear that the intersection of the convex hull with a boundary face is even a polytope. Rather than computing the convex hull explicitly, it might be easier to find an algorithm that tests whether a point is in the convex hull or not. This would be sufficient for most applications, including computing a geometric centre by peeling convex hulls.

## 7 Acknowledgements

The authors thank Sean Skwerer for the example showing convex hulls of 3 points can be 3-dimensional (Figure 7), and Aasa Feragen, Steve Marron, Ezra Miller, Vinayak Pathak, Scott Provan, and Sean Skwerer for helpful discussions about convex hulls in tree space. MO acknowledges the support of the Fields Institute. Research supported by NSERC, the Natural Sciences and Engineering Research Council of Canada.

## References

- [1] R. K. Ahuja, T. L. Magnanti, and J. B. Orlin. *Network Flows: Theory, Algorithms, and Applications*. Prentice Hall, Englewood Cliffs, NJ, 1993.
- [2] F. Ardila, M. Owen, and S. Sullivant. Geodesics in CAT(0) cubical complexes. *Advances in Applied Mathematics* 48(1):142–163, 2012.
- [3] M. Bacak. Computing medians and means in Hadamard spaces. *SIAM Journal on Optimization* 24(3):1542–1566, 2014.
- [4] M. Bacak. *Convex analysis and optimization in Hadamard spaces*, vol. 22. Walter de Gruyter GmbH & Co KG, 2014.
- [5] D. Barden, H. Le, and M. Owen. Limiting behaviour of Fréchet means in the space of phylogenetic trees. *arXiv preprint arXiv:1409.7602*, 2014.
- [6] M. Berger. *A panoramic view of Riemannian geometry*. Springer Science & Business Media, 2003.
- [7] L. J. Billera, S. P. Holmes, and K. Vogtmann. Geometry of the space of phylogenetic trees. *Advances in Applied Mathematics* 27(4):733–767, 2001.
- [8] A. Borbély. Some results on the convex hull of finitely many convex sets. *Proceedings of the American Mathematical Society* 126(5):1515–1525, 1998.
- [9] B. H. Bowditch. Some results on the geometry of convex hulls in manifolds of pinched negative curvature. *Commentarii Mathematici Helvetici* 69(1):49–81, 1994.
- [10] M. R. Bridson and A. Haefliger. *Metric spaces of non-positive curvature*, vol. 319. Springer Science & Business Media, 1999.

- [11] T. M. Chan. Optimal output-sensitive convex hull algorithms in two and three dimensions. *Discrete & Computational Geometry* 16(4):361–368, 1996.
- [12] B. Chazelle. Triangulating a simple polygon in linear time. *Discrete & Computational Geometry* 6:485–524, 1991, doi:10.1007/BF02574703.
- [13] B. Chazelle. An optimal convex hull algorithm in any fixed dimension. *Discrete and Computational Geometry* 10(1):377–409, 1993.
- [14] J. Chen and Y. Han. Shortest paths on a polyhedron, Part I: Computing shortest paths. *International Journal of Computational Geometry & Applications* 6(02):127–144, 1996, doi:10.1142/S0218195996000095.
- [15] V. Chepoi. Graphs of some CAT(0) complexes. *Advances in Applied Mathematics* 24(2):125–179, 2000.
- [16] V. Chepoi, F. F. Dragan, and Y. Vaxès. Distance and routing labeling schemes for non-positively curved plane graphs. *Journal of Algorithms* 61(2):60–88, 2006.
- [17] V. Chepoi and D. Maftuleac. Shortest path problem in rectangular complexes of global nonpositive curvature. *Computational Geometry* 46(1):51–64, 2013, doi:10.1016/j.comgeo.2012.04.002.
- [18] M. Dror, A. Efrat, A. Lubiw, and J. S. Mitchell. Touring a sequence of polygons. *Proceedings of the 35th Annual ACM Symposium on Theory of Computing (STOC)*, pp. 473–482, 2003, doi:10.1145/780542.780612.
- [19] M. Elder and J. McCammond. CAT(0) is an algorithmic property. *Geometriae Dedicata* 107(1):25–46, 2004, doi:10.1023/B:GEOM.0000049096.63639.e3.
- [20] J. Felsenstein. Confidence limits on phylogenies: an approach using the bootstrap. *Evolution* pp. 783–791, 1985.
- [21] P. Fletcher, J. Moeller, J. Phillips, and S. Venkatasubramanian. Horoball hulls and extents in positive definite space. *Algorithms and Data Structures*, pp. 386–398. Springer Berlin Heidelberg, Lecture Notes in Computer Science 6844, 2011, doi:10.1007/978-3-642-22300-6\_33.
- [22] R. Ghrist and V. Peterson. The geometry and topology of reconfiguration. *Advances in applied mathematics* 38(3):302–323, 2007.
- [23] M. Gromov. Hyperbolic groups. *Essays in Group Theory*, pp. 75–263. Springer New York, Mathematical Sciences Research Institute Publications 8, 1987, doi:10.1007/978-1-4613-9586-7\_3.
- [24] L. Guibas, J. Hershberger, D. Leven, M. Sharir, and R. E. Tarjan. Linear-time algorithms for visibility and shortest path problems inside triangulated simple polygons. *Algorithmica* 2(1-4):209–233, 1987, doi:10.1007/BF01840360.



- [25] L. J. Guibas and J. Hershberger. Optimal shortest path queries in a simple polygon. *Journal of Computer and System Sciences* 39(2):126 – 152, 1989, doi:10.1016/0022-0000(89)90041-X.
- [26] F. Haglund and D. T. Wise. Special cube complexes. *Geometric and Functional Analysis* 17(5):1551–1620, 2008.
- [27] J. Hershberger and J. Snoeyink. Computing minimum length paths of a given homotopy class. *Computational Geometry* 4(2):63–97, 1994, doi:10.1016/0925-7721(94)90010-8.
- [28] J. Hershberger and S. Suri. An optimal algorithm for euclidean shortest paths in the plane. *SIAM J. Comput* 28:2215–2256, 1997.
- [29] S. Holmes. Statistical approach to tests involving phylogenies. *Mathematics of evolution and phylogeny. Oxford University Press, Oxford, UK* pp. 91–120, 2005.
- [30] M. Ishaque and C. D. Tóth. Relative convex hulls in semi-dynamic arrangements. *Algorithmica* 68(2):448–482, 2014, doi:10.1007/s00453-012-9679-6.
- [31] N. Karmarkar. A new polynomial-time algorithm for linear programming. *Proceedings of the sixteenth annual ACM symposium on Theory of computing*, pp. 302–311, 1984.
- [32] L. G. Khachiyan. Polynomial algorithms in linear programming. *USSR Computational Mathematics and Mathematical Physics* 20(1):53–72, 1980.
- [33] D. G. Kirkpatrick and R. Seidel. The ultimate planar convex hull algorithm? *SIAM Journal on Computing* 15(1):287–299, 1986.
- [34] D. Lee and F. P. Preparata. Euclidean shortest paths in the presence of rectilinear barriers. *Networks* 14(3):393–410, 1984, doi:10.1002/net.3230140304.
- [35] D.-T. Lee and B. J. Schachter. Two algorithms for constructing a Delaunay triangulation. *International Journal of Computer and Information Sciences* 9(3):219–242, 1980.
- [36] B. Lin, B. Sturmfels, X. Tang, and R. Yoshida. Convexity in tree spaces. *arXiv preprint arXiv:1510.08797*, 2015.
- [37] D. Maftuleac. Algorithms for distance problems in planar complexes of global non-positive curvature. *International Journal of Computational Geometry & Applications* 24(01):1–38, 2014, doi:10.1142/S0218195914500010.
- [38] E. Miller, M. Owen, and J. S. Provan. Polyhedral computational geometry for averaging metric phylogenetic trees. *Advances in Applied Mathematics* 68:51–91, 2015.
- [39] J. S. Mitchell. Geometric shortest paths and network optimization. *Handbook of Computational Geometry*, pp. 633–701. Elsevier Science Publishers B.V. North-Holland, 1998.

- [40] J. S. Mitchell, D. M. Mount, and C. H. Papadimitriou. The discrete geodesic problem. *SIAM Journal on Computing* 16(4):647–668, 1987.
- [41] D. M. Mount. Storing the subdivision of a polyhedral surface. *Discrete & Computational Geometry* 2(1):153–174, 1987, doi:10.1007/BF02187877.
- [42] T. M. Nye. An algorithm for constructing principal geodesics in phylogenetic treespace. *Computational Biology and Bioinformatics, IEEE/ACM Transactions on* 11(2):304–315, 2014.
- [43] M. Owen and J. S. Provan. A fast algorithm for computing geodesic distances in tree space. *IEEE/ACM Transactions on Computational Biology and Bioinformatics (TCBB)* 8(1):2–13, 2011.
- [44] F. Ronquist and J. P. Huelsenbeck. MrBayes 3: Bayesian phylogenetic inference under mixed models. *Bioinformatics* 19(12):1572–1574, 2003.
- [45] R. Seidel. Convex hull computations. *Handbook of Discrete and Computational Geometry (2nd edition)*, pp. 495–512. CRC Press, Inc., 2004.
- [46] G. Toussaint. An optimal algorithm for computing the relative convex hull of a set of points in a polygon. *Signal Processing III: Theories and Applications, Proc. EURASIP-86, Part 2*, pp. 853–856, 1986.
- [47] G. Toussaint. Computing geodesic properties inside a simple polygon. *Rev. Intell. Artif.* 3:9–42, 1989.
- [48] J. W. Tukey. Mathematics and the picturing of data. *Proceedings of the International Congress of Mathematicians*, vol. 2, pp. 523–531, 1975.
- [49] G. U. Yule. A mathematical theory of evolution, based on the conclusions of Dr. JC Willis, FRS. *Philosophical Transactions of the Royal Society of London. Series B, Containing Papers of a Biological Character* pp. 21–87, 1925.